Master of Science Thesis

# Hybrid Eulerian-Lagrangian Vortex Particle Method

## A fast and accurate numerical method for 2D Vertical-Axis Wind Turbine

**L. Manickathan B.Sc.**

Date TBD

Faculty of Aerospace Engineering · Delft University of Technology

# Hybrid Eulerian-Lagrangian Vortex Particle Method

## A fast and accurate numerical method for 2D Vertical-Axis Wind Turbine

Master of Science Thesis

For obtaining the degree of Master of Science in Aerospace Engineering at Delft University of Technology

L. Manickathan B.Sc.

Date TBD

Faculty of Aerospace Engineering · Delft University of Technology

TU Delft Delft University of Technology

Delft University Of Technology
Department Of
Aerodynamics and Wind Energy

The undersigned hereby certify that they have read and recommend to the Faculty of Aerospace Engineering for acceptance a thesis entitled **"Hybrid Eulerian-Lagrangian Vortex Particle Method"** by **L. Manickathan B.Sc.** in partial fulfillment of the requirements for the degree of **Master of Science**.

Dated: Date TBD

Head of department: ______________________
prof.dr.ir. G.J.W. van Bussel

Academic Supervisor: ______________________
dr.ir. C.J. Simao Ferreira

Academic Supervisor: ______________________
dr.ir. A. Palha da Silva Clerigo

Industrial Supervisor: ______________________
prof.dr.ir. I. Bennett

# Summary

This is the summary of the thesis.

# Acknowledgements

I wish to thank the following persons…

Delft, The Netherlands L. Manickathan B.Sc.
Date TBD

# Contents

# List of Figures

# List of Tables

# Nomenclature

## Latin Symbols

| | | |
|---|---|---|
| $h$ | Nominal particle spacing | $[m]$ |
| $\mathbf{K}$ | Biot-Savart kernel | $[-]$ |
| $\mathbf{K}_\sigma$ | Vortex blob kernel | $[-]$ |
| $N_p$ | Number of particles | $[-]$ |
| overlap | Overlap ratio of the blobs | $[-]$ |
| $p$ | Pressure | [Pa] |
| $t$ | Time | $[s]$ |
| $\mathbf{u}$ | Velocity | $[m \cdot s^{-1}]$ |
| $\mathbf{u}^h$ | Discrete velocity | $[m \cdot s^{-1}]$ |
| $\mathbf{u}_\infty$ | Free-stream velocity | $[m \cdot s^{-1}]$ |
| $\mathbf{u}_\phi$ | Potential velocity | $[m \cdot s^{-1}]$ |
| $\mathbf{u}_\omega$ | Vortical velocity | $[m \cdot s^{-1}]$ |
| $\mathbf{x}$ | Position vector | $[m]$ |
| $\mathbf{x}_p$ | Position vector of the particle | $[m]$ |

## Greek Symbols

| | | |
|---|---|---|
| $\zeta_\sigma$ | Smooth cut-off function of the blob | $[-]$ |
| $\Gamma$ | Circulation | $[m^2 \cdot s^{-1}]$ |
| $\Gamma_p$ | Circulation of the particle | $[m^2 \cdot s^{-1}]$ |
| $\nu$ | Kinematic viscosity | $[m^2 \cdot s^{-1}]$ |

|  |  |  |
|---|---|---|
| $\rho$ | Density | $[kg \cdot m^{-3}]$ |
| $\sigma$ | Core size | $[m]$ |
| $\omega$ | Vorticity | $[s^{-1}]$ |
| $\omega^h$ | Discrete vorticity field | $[s^{-1}]$ |

# Abbreviations

|  |  |
|---|---|
| **FMM** | Fast-Multipole Method |
| **GPU** | Graphics Processing Units |
| **PSE** | Particle Strength Exchange |
| **VAWT** | Vertical-Axis Wind Turbine |
| **VPM** | Vortex Particle Method |
| **VRM** | Vortex Redistribution Method |

# Chapter 1

# Introduction

Conventional energy resources such as fossil fuels and nuclear energy are not only limited supply but also pose adhere effects on the environment. Therefore, we are striving to find a cheap and renewable source of energy. Wind energy is such source of energy and is therefore getting more popular and also become more affordable and novel renewable technologies such as Vertical-Axis Wind Turbine (VAWT) is now an interested research field.

Vertical-Axis Wind turbines are unlike the normal wind turbine. Typical wind turbines are mounted on a mast away from the ground and generates energy by spinning normal to the ground. However, a VAWT spins parallel to the ground with its hub located at the ground [14]. The advantages of the vertical axis wind turbine are what makes them ideal for a source of renewable energy. As the turbine is located at the ground (unlike the Horizontal-Axis Wind Turbine), it is easily accessible and can be easily maintained. The second main advantage of the VAWT is the way it dissipates its wake [6] [12]. As the fluid past the turbine is more turbulent, the flow is able to smooth out much earlier. This means that it possible to places VAWTs much closer to each other is so in future this means that a VAWT farm can potentially give more power per area. Furthermore, operate independent of the flow direction and can operate at low wind speeds (low tip-speed ratios).

## 1.1 Motivation and Goal

However, with these advantages also comes drawbacks. As the blades passes through its own dirty air (the wake), complex wake-body interactions take places. These have adhere effect on the blade structure and therefore is more susceptible to fatigue. This happens because the blades are constantly pitching in front the free-stream flow and complex flow behaviour such as dynamic stall and constant vortex shedding occurs [10]. This complex fluid behaviours makes it hard to predict the performance of a VAWT and this is one of the reasons why VAWTs are not mainstream. In addition, as the VAWT operates at large Reynolds number, accurate numerical methods are computationally very expensive. Therefore, it is vital to have a good understanding of the flow structure evolution and the wake generation of the VAWT using not only an efficient method, but also an accurate one.

To summarize, we are now able to formulate a research goal. The key interest of this project is to develop an efficient, reliable, and an accurate numerical method for modelling the flow around a 2D VAWT. For now, only 2D problems are considered because 3D method is build upon the methodology of the 2D. Thus, once the 2D methodology is made, a 3D numerical method should be a straightforward extension.

Furthermore, the numerical method efficient at capturing both the near-wake phenomenons such as the vortex shedding, dynamic stall, & the wake-body interaction, and should be able to capture the large scale flow structure such as the evolution of the VAWT wake. From this criterias, we are able to formulate the research question.

## 1.2 Research Aim and Plan

**Research Question:** *Is it possible to develop a numerical method that is both efficient at capturing the small-scale phenomenons and the large scale phenomenons? Is is possible to apply this to a 2D VAWT?*

**Research aim and plan:**

- Develop a numerical method for capturing small-scale phenomenons and large scale phenomenons.
- Ensure this tool is efficient, reliable, and accurate.
- Verify, Validate the tools with model problems.
- Apply the model to the 2D flow of VAWT.

With the above formulate research question, aim and plan we are able to thoroughly perform the literature study to determine whether the research goal stated here is feasible. Finally, this report will answer why a Hybrid Eulerian-Lagrangian Vortex Particle Method will be used to the achieved the goals.

## 1.3 Introduction to Hybrid Eulerian-Lagrangian Vortex Particle Method

### 1.3.1 Advantage of domain decomposition

### 1.3.2 Methodology

## 1.4 Thesis Outline

Chapter 2

# Lagrangian Domain: Vortex Particle Method

## 2.1 Introduction to Vortex Particle Method

Vortex Particle Method (VPM) is a branch of computational fluid dynamics that deals with the evolution of the vorticity of the fluid in a lagrangian description. Typically, the fluid is viewed at a fixed window where it is described as a function of space $\mathbf{x}$ and time $t$. However, the lagrangian point of view regards the fluid as a collection of the particles carrying the property of the fluid.

Unlike the typical eulerian method that require discretization of all the fluid domain, VPM only needs fluid elements where there is vorticity. This means that the VPM are inherently auto-adaptive method that only simulated the flow of interest. Furthermore, with the computational acceleration methods such as Fast-Multipole Method (FMM) and parallel computation on Graphics Processing Units (GPU) , VPM can be more efficient that typical eulerian methods.

### 2.1.1 Vorticity

Vorticity $\omega$, the governing element of vortex particle method, is defined as

$$\omega = \Delta \times \mathbf{u}, \tag{2.1}$$

where $\mathbf{u}$ is the velocity. The circulation $\Gamma$ is defined as

$$\Gamma = \int_L \mathbf{u} \cdot d\mathbf{r} = \int_S \omega \cdot \mathbf{n}\; dS, \tag{2.2}$$

by the stokes theorem, as represents the integral vorticity of the domain, figure 2.1

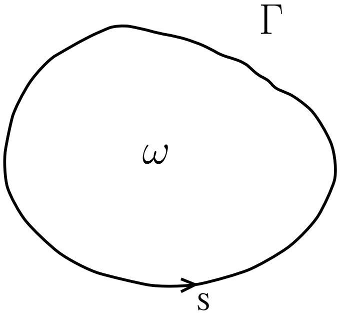

**Figure 2.1:** Circulation of the fluid

### 2.1.2 Velocity-vorticity formulation of the Navier-Stokes equations

The governing equation of the vortex particle method is velocity-vorticity $\mathbf{u}-\omega$ formulation of the Navier-Stokes equations [4]. The 2-D incompressible Navier-Stokes momentum equation is given as

$$\frac{\partial \mathbf{u}}{\partial t}+\mathbf{u}\cdot\nabla\mathbf{u}=-\frac{1}{\rho}\nabla p+\nu\nabla^2\mathbf{u}, \tag{2.3}$$

relating the velocity field $\mathbf{u}\left(\mathbf{x},t\right)$ to the pressure field $\mathbf{p}\left(\mathbf{x},\mathbf{t}\right)$, the kinematic viscosity $\nu$ and density $\rho$. Furthermore, we also have to satisfy the incompressibility constraint given as

$$\nabla\cdot\mathbf{u}=0. \tag{2.4}$$

To attain the velocity-vorticity formulation, we should take the curl of the velocity-pressure $\mathbf{u}-p$ formulation of the Navier-Stokes equation. Taking the curl of the momentum equation 2.3, we get the vorticity transport equation

$$\frac{\partial \omega}{\partial t}+\mathbf{u}\cdot\nabla\omega=\nu\nabla^2\omega, \tag{2.5}$$

which only relates the vorticity to the velocity enabling us to neglect the pressure field. Note that as we are dealing with the two dimensional flow, we neglected the stretching term.

### 2.1.3 Viscous splitting algorithm

Vortex particle method was initially used to model the evolution of incompressible, inviscid flows. However, in order to simulate a real flow, we must also deal with the viscous behaviour of the fluid. Chorin [3] has shown that using the viscous splitting algorithm, it is possible to simulate a viscous flow.

The viscous splitting algorithm is basically a fractional step method, where the viscous and the inviscid part of the transport equation is dealt in two subsequent steps,

- Sub-step 1: convection

$$\frac{\partial \omega}{\partial t} + \mathbf{u} \cdot \nabla \omega = 0; \tag{2.6}$$

- Sub-step 2: diffusion

$$\frac{\partial \omega}{\partial t} = \nu \nabla^2 \omega. \tag{2.7}$$

The first sub-step of the evolution deals with the convection of the vorticity. Note that, by convection we imply the advection of the vorticity field where the diffusion process is neglected. The second sub-step is where we deals with the diffusion of the vorticity field.

There are several advantage to this type of evolution. As the convection and diffusion are handled separately, there is minimum dispersion during the convection and furthermore, the is no restriction of the advection CFL number [13].

There are many ways of dealing with the diffusion of the vorticity field. During this project, we use a modified interpolation kernel [13] that can simultaneously treat diffusion and remesh the vortex particles, see section 2.3.

## 2.2 Spatial Discretization: Generation of Vortex Blobs

In order to deal with the vorticity field, we must first discretize the vorticity to vortex particles. Vortex blobs have been first introduced by Chorin and is a mollified particle carrying the local circulation. Vortex blobs describes a smooth vorticity field and are ideal because of it does not cause singularity issues when particles approach each other.

!!! check for consistency, continuity !!!

### 2.2.1 Biot-Savart law

The velocity field can be decomposed using the Helmholtz decomposition, given as

$$\mathbf{u} = \mathbf{u}_\omega + \mathbf{u}_\phi, \tag{2.8}$$

where $\mathbf{u}_\omega$ is the rotational component of the velocity and $\mathbf{u}_\phi$ is the irrotational component. solenoidal and potential velocity respectively. In an unbounded flow we have $\mathbf{u}_\phi$ equal to the free-stream velocity $\mathbf{u}_\infty$. For bounded flow, we must include the presence of the body, see section 2.4.

The velocity can be related to the vorticity using the Biot-Savart law

$$\mathbf{u}_\omega = \mathbf{K} \star \omega, \tag{2.9}$$

where the $\star$ represents convolution of the 2-D kernel $\mathbf{K}$ given by

$$\mathbf{K} = \frac{1}{2\pi \left|\mathbf{x}\right|^2} \left(-x_2, x_1\right). \tag{2.10}$$

### 2.2.2 Discrete form of vorticity field

The spatial discretization of the fluid domain is done through $N$ quadrature points. With the Biot-Savart law, we can treat these quadratures are discrete particles carrying the local quantities. The discrete vorticity field is given as

$$\omega\left(\mathbf{x},t\right) \simeq \omega^{h}\left(\mathbf{x},t\right) = \sum_{p} \alpha_{p}\left(t\right)\delta\left[\mathbf{x}-\mathbf{x}_{p}\left(t\right)\right], \tag{2.11}$$

where $\alpha_p$ is the estimate of the circulation around the particle $\mathbf{x}_p$ with core size $\sigma$. We must not that $\omega^h$ is an approximately equal to $\omega$ of the fluid due to the discretization.

The discrete form of the velocity is therefore written as

$$\mathbf{u} \simeq \mathbf{u}^{h} = \sum_{p} \mathbf{K}\left[\mathbf{x}-\mathbf{x}_{p}\left(t\right)\right]\alpha_{p}\left(t\right). \tag{2.12}$$

Thus the discrete vorticity field is an $N$-body problem inducing velocity on each and implicitly evolving the vorticity field. This is one of the advantage of the vortex particle method as there are many ways to efficiently treat the problem. The $N$-body problem can be parallelized and can be accelerated using fast summation methods such as FMM, see 2.5.

However, like all $N$-body problem, equation 2.10 has a singularity when the particles approach each other and can result in numerical instability. To overcome this we can mollify the kernel, removing the singularity.

### 2.2.3 Convection of vortex blobs

In the discrete of the convection equation 2.6 of the viscous-splitting algorithm, the is solved as system of ODEs, where

$$\frac{\mathrm{d}\mathbf{x}_p}{\mathrm{d}t} = \mathbf{u}\left(\mathbf{x}_p\right), \tag{2.13}$$

with

$$\frac{\mathrm{d}\Gamma_p}{\mathrm{d}t} = 0. \tag{2.14}$$

As the diffusion is done at the next sub-step, we have to ensure that the circulation is conserved.

### 2.2.4 Mollified vortex kernels

A vortex particle with a mollified core, non-zero core-size, is referred to as vortex blobs. The advantage of the vortex blobs is that the with a smooth distribution of the vorticity, the singularity disappears and so numerical instability does not happen when blobs get too close to each other. An ideal choice for a cutoff function is a Gaussian distribution, figure 2.2.

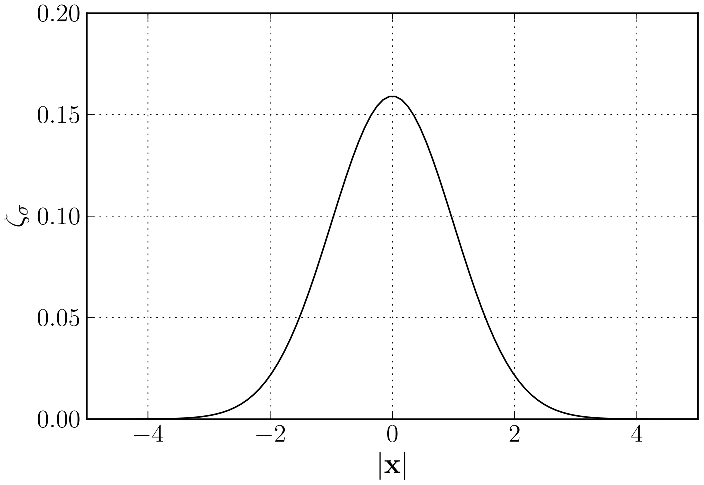

**Figure 2.2:** Vortex blob with Gaussian distribution: $[k = 2,\ \sigma = 1.0]$

Gaussian kernels satisfy the requirement for smooth distribution ad decays quickly and is defined as

$$\zeta_\sigma = \frac{1}{k\pi\sigma^2}\exp\left(\frac{-|\mathbf{x}|}{k\sigma^2}\right), \tag{2.15}$$

where $k$ is 1, 2 or 4 and determines the width of the kernel, $\sigma$ is core-size of the blob. Note that smoothing function is chosen such that $\int\zeta = 1$, ensuring the conservation of circulation when mollified. So, using a smooth cut-off function $\zeta_\sigma$, the mollified kernel $\mathbf{K}_\sigma$ is given as

$$\mathbf{K}_\sigma = \mathbf{K} \star \zeta_\sigma. \tag{2.16}$$

The mollified vorticity field, represented by vortex blobs is given as

$$\omega^h(\mathbf{x}, t) = \sum_p \alpha_p(t)\,\zeta_\sigma\left[\mathbf{x} - \mathbf{x}_p(t)\right], \tag{2.17}$$

now representing the mollified vorticity field and equivalently, the mollified velocity field is given as

$$\mathbf{u}^h(\mathbf{x}, t) = \sum_p \mathbf{K}_\sigma\left[\mathbf{x} - \mathbf{x}_p(t)\right]\alpha_p(t). \tag{2.18}$$

Koumoutsakos and Chorin [4], have shown that for proper communication between the particle, the particle needs to overlap,

$$\text{overlap} = \frac{\sigma}{h}, \tag{2.19}$$

where $h$ is the nominal particle spacing, figure 2.3. If the particles fail to overlap, vortex blobs will also fail to recover the vorticity field. Such problems occurs when blobs are clustered due to high flow strain, leading to lagrangian grid distorting and must be treated, see section 2.2.6.

### 2.2.5 Vortex blob initialization

Now the question arises on how to initialize the particle's circulation strengths $\alpha_p$. A common approach that is used is to estimate the particles strength is to say that

$$\alpha_p = \omega_p \cdot h^2. \tag{2.20}$$

This might seem like a valid assumption as the circulation of a given area is the integral of the vorticity in the area, equation 2.2, however this is no longer valid when regularizing the vorticity field using mollified gaussian kernels, equation 2.17. Barba and Rossi [1], has described this problem as gaussian blurring of the original vorticity field. Even though the particle have acquired the correct circulation strengths (i.e the local property), when evaluating the mollified vorticity field, we see that there is a mismatch in the evaluated vorticity field, figure 2.4.

Another way of viewing this characteristic is say the conservation of circulation is only valid globally, but not locally. A common standard for recovering the initial vorticity field is perform the Beale's method [2].

#### Beale's Iterative Method

The Beale's method is particle circulation processing scheme where the circulation of the particles are modified such that the mollified vorticity field matches the indented vorticity field. The recovery of the vorticity field is done by performing a discrete deconvolution,

$$\sum_{j}^{N} \beta_j \zeta_\sigma \left(\mathbf{x}_i - \mathbf{x}_j\right) = \omega_i, \tag{2.21}$$

where $\beta_j$ is the circulation of the particles at positions $\mathbf{x}_j$ such that it matches the exact vorticity $\omega_i$ at the position $\mathbf{x}_i$ that we are evaluating. As we are try to solve for a $N$

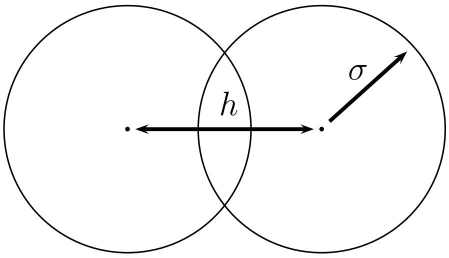

**Figure 2.3:** Vortex blob with overlap $\sigma/h$

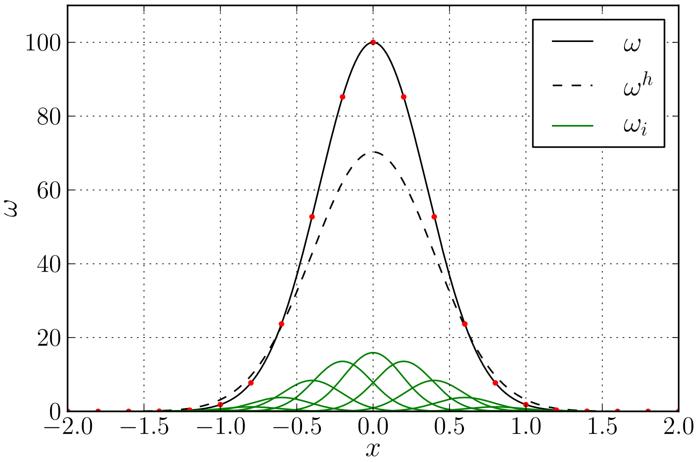

**Figure 2.4:** Mollified vorticity field of an arbitrary vorticity function with $\text{overlap} = 1.0$, $\sigma = 0.19$, $h = 0.19$. Vortex blob strength has been assigned by equation 2.20, sampling at exact vorticity [●, red dot]. Figure depicts exact vorticity distribution $\omega$ [—, solid], vorticity field of each blob $\omega_i$ [—, green dashed], the mollified vorticity field $\omega^h$ [- -, dashed].

unknown problem, we must set up a $N$ system of equations. Multiplying both sides with the area associated to the blobs, we get

$$\mathbf{A}_{ij}\beta_j = \alpha_i^{\text{exact}}, \tag{2.22}$$

where

$$\mathbf{A}_{ij} = \zeta_\sigma \left(\mathbf{x}_i - \mathbf{x}_j\right) \cdot h^2 \tag{2.23}$$

is a $N \times N$ matrix containing the weights of the influence of each particle on each other. This matrix can be constructed by setting the $\Gamma$ to one and determine the induced vorticity on each other. Furthermore, we see that it is not feasible to directly invert the matrix when we have large set of blobs but most importantly as the matrix $\mathbf{A}$ is severly ill-conditioned [11], it should not be directly inverted. Beale's proposition to this problem was to iteratively solve for the solution,

$$\beta_j^{n+1} = \alpha_i + \beta_i^n - \mathbf{A}_{ij} \cdot \beta_j^n \tag{2.24}$$

We see that with just two iterations, the error between the mollified and exact vorticity field reduces drastically, figure 2.5. Koumoutsakos and Cottet [4], had shown that there was a drastic improvement in the velocity with just two to three iterations. However, we see that the cell vorticity of the blobs, directly evaluated from the particle strengths, equation 2.20, are more peaky and no longer matches the exact vorticity.

During the hybrid coupling algorithm, we see that this is the central source of coupling error between the eulerian and the lagrangian method, section **??**. When performing the hybrid coupling, we need to recover the vorticity field transfered from the eulerian domain

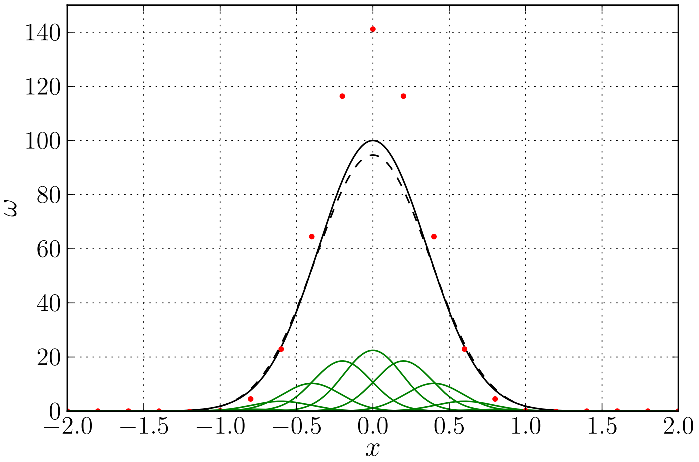

**Figure 2.5:** Mollified vorticity field after two Beale's iteration, overlap $= 1.0$, $\sigma = 0.19$, $h = 0.19$. Figure depicts exact vorticity distribution $\omega$ [—, solid], vorticity field of each blob $\omega_i$ [—, green dashed], the mollified vorticity field $\omega^h$ [- -, dashed].

to the lagrangian domain in every step. So, beale's correction is not a viable solution for the hybrid method. Thus there is a need for an alternate method of recovering the vorticity field.

!!! add the reference to hybrid !!!

### Convergence of particle discretization

An alternate, temporary method to reduce the gaussian blurring of the vorticity field is to reduce the overlap (i.e. increase the overlap ratio) of the vortex blobs and to the increase the spatial resolution.

Figure 2.6 shows mollified vorticity field results from modifying the spatial resolution parameters. Figure 2.6a shows the convergence of the mollified vorticity field $\omega^h$ to

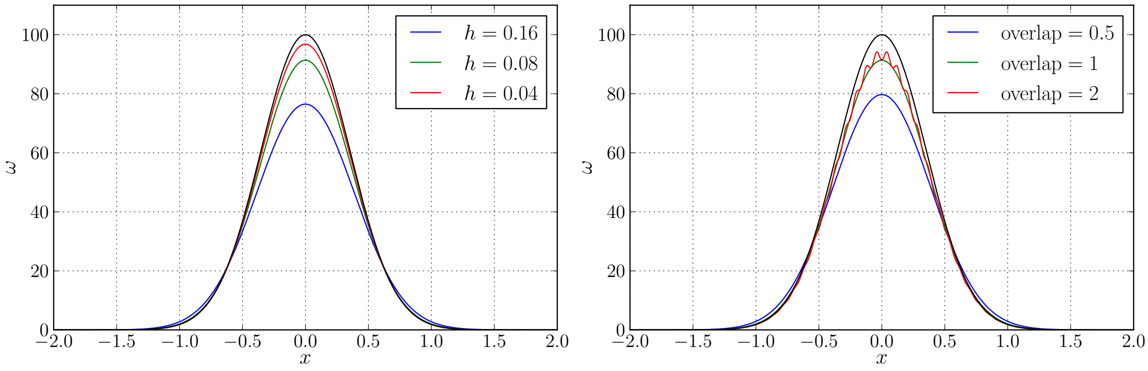

**(a)** Convergence of $h$ with overlap $= 1.0$

**(b)** Convergence of overlap with $h = 0.08$

**Figure 2.6:** Convergence of vorticity by modifying the spatial resolution. Figure depicts exact vorticity field $\omega$ with [—, black] and various resolutions.

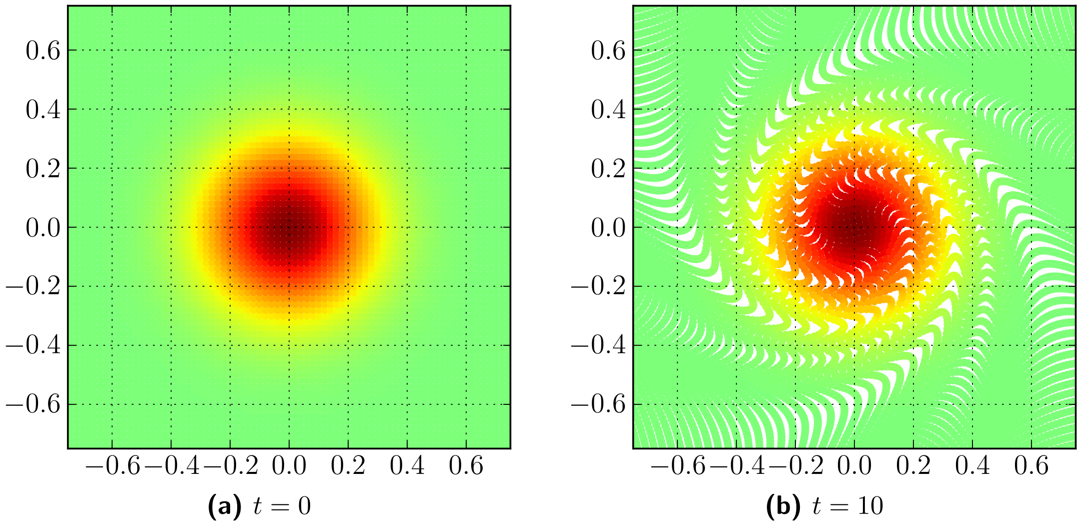

**(a)** $t = 0$ **(b)** $t = 10$

**Figure 2.7:** Lagrangian distortion of the vortex blobs after 100 steps. The initial vorticity field $\omega\left(\mathbf{x},0\right) = \exp\left(-12\left|\mathbf{x}\right|\right)$ with $\Delta t = 0.1$, $\sigma = 0.02$ and overlap $= 1.0$. Figure depicts the initial and the final distribution of the vortex blobs.

the exact vorticity field $\omega$ by reducing the nominal particle spacing $h$. The blobs have overlap $= 1$ and so the blob core-size $\sigma$ is equal to $h$. We see that as you reduce the size of the blob and increase the number of particles, the mollified vorticity converges to the exact vorticity. Therefore, an alternate method of reducing the gaussian blurring is to increase the spatial resolution.

Furthermore, we could also adjust the overlap of the blobs, figure 2.6b. The $\sigma$ and $h$ of the blob is 0.08 and we see that increasing overlap number (i.e reducing the overlap), helps us to recover the original vorticity field. However, as explained by Koumoutsakos [4], if the overlap is too low, we lose the smooth recovery of the vorticity field. This is apparent when overlap $= 2.0$, where we see that the mollified vorticity field is fluctuation.

Therefore, for the hybrid coupling, we set overlap $= 1.0$ and maximize the spatial resolution at the coupling zone.

### 2.2.6 Remeshing scheme: Treating lagrangian grid distortion

During the convection step, we see that another source of error in the vorticity field is the lagrangian grid distortion. As we have seen before, when the vortex blobs fails to overlap, we are no longer able to reconstruct the correct the vorticity field, figure 2.6b. During the convection, due to the high strains in the fluid, the vortex blobs tent to clump together and creates regions where no vortex blobs are found, reducing the overlap of the blobs, figure 2.7.

We see that due to clustering of the vortex blobs, it fails to reproduce the correct vorticity field. A common strategy to overcome this problem is to remesh the vortex blobs to a uniform grid, so that we have a continuous vorticity field.

However, when transfering the vorticity from the old deformed grid to the new lagrangian uniform grid, we must satisfy the conservation laws of vorticity field. The interpola-

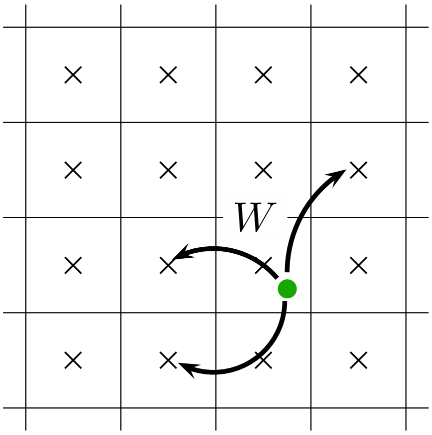

**Figure 2.8:** Interpolation of vortex blob (●, green) on the uniform grid.

tion methods is based on the conservation of linear impulse which directly implies the conservation of the total circulation [4]. The transfer of the particle strengths is given as,

$$\alpha_p = \sum_q \tilde{\alpha}_q W \left( \frac{x_p - \tilde{x}_q}{h} \right), \tag{2.25}$$

where the strengths of the particles $\tilde{\alpha}_q$ of the distorted lagrangian grid $\tilde{x}_q$ is transfered to the regular lagrangian grid $x_p$ using the interpolation kernel, weighted $W$, giving us the remeshing particle strengths $\alpha_p$. The transfer of strengths of one particles to it's interpolation nodes can be seen in figure 2.8.

### $\mathrm{M}_4'$ interpolation kernel

For lagrangian problem, we use the efficient interpolation kernel that has been used to reconstruct a smooth distribution interpolation, the $\mathrm{M}_4'$ interpolation kernel, introduced by Monaghan [8]. In one dimension it is given as,

$$\mathrm{M'}_4(\xi) = \begin{cases} 1 - \frac{5\xi^2}{2} + \frac{3|\xi|^3}{2} & |\xi| < 1, \\ \frac{1}{2}(2 - |\xi|)^2 (1 - |\xi|) & 1 \leq |\xi| < 2, \\ 0 & 2 \leq |\xi|, \end{cases} \tag{2.26}$$

where $\xi = x_p - x$ is the distance of the particle to the interpolation nodes. The $\mathrm{M'}_4$ is a third-order accurate piecewise smooth B-spline kernel, where $m = 4$ giving it 4 support nodes, figure 2.9. For the two dimensional problem that we have, the 2-D interpolation formula is simply tensor product of the 1-D interpolation kernel equation 2.26, and results in $4^2 = 16$ support nodes, figure 2.8.

The interpolation kernel achieves the third-order accuracy as it conserves linear and the angular momentum of the vortex. Koumoutsakos [7] has investigated the drawback of the employing the remeshing strategy and have shown that there is approximately 4% decay in enstrophy of the flow due to sub-grid dissipation.

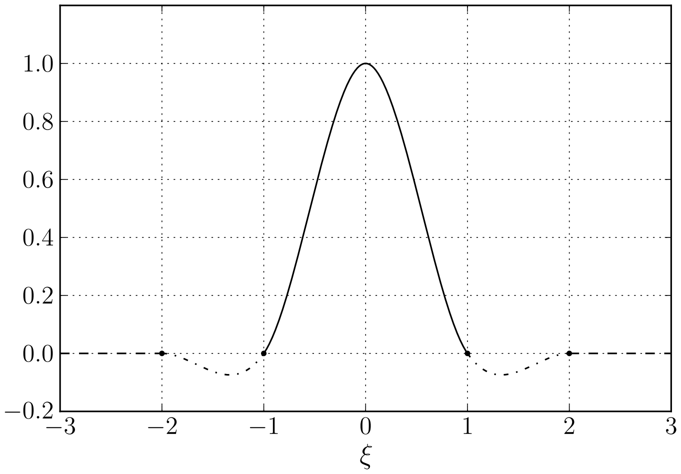

**Figure 2.9:** Interpolation kernel

## 2.3 Diffusion of Vortex Methods

Chorin initially employed a random walk method, however this method suffers some limitations in accuracy and since then several methods have been introduced that can be used to simulate the diffusion. Particle Strength Exchange (PSE) method [5], is an algorithm to treat diffusion by exchange of vortex element strengths. Vortex Redistribution Method (VRM) [9] models diffusion by distributing the fraction of circulation of the vortex elements to the neighbouring vortices.

### 2.3.1 Vorticity diffusion techniques

### 2.3.2 Modified remeshing for treating diffusion

The diffusion method that is applied here has been proposed by Shankar and Van Dommelen [9] and the modified $\mathrm{M}'_4$ interpolation kernel has been derived by Ghoniem and Wee [13] and was also applied by Speck [?]. The diffusion is simulated by the modified interpolation kernel during the remeshing process. During remeshing, the heat equation is satisfied by transferring the correct fraction of circulation to produce the proper amount of diffusion. The $\mathrm{M}'_4$ kernel was modified to treat the diffusion and is given by:

$$\mathrm{M}'_4\left(\xi, c\right) = \begin{cases} 1 - \frac{5\xi^2}{2} + \frac{3|\xi|^3}{2} - c^2\left(2 - 9\xi^2 + 6|\xi|^3\right) & |\xi| < 1, \\ \frac{1}{2}(2-|\xi|)^2\left(1-|\xi|\right) - c^2(2-|\xi|)^2\left(1 - 2\left|\xi\right|\right) & 1 \le |\xi| < 2, \\ 0 & 2 \le \left|\xi\right|, \end{cases} \tag{2.27}$$

where

$$c^2 = \frac{\nu \Delta t_d}{h^2}, \tag{2.28}$$

and corresponds to the transfer quantity for diffusion. The $\nu$ denotes the viscosity of the fluid, $t_d$ is the diffusion time step and $\Delta x$ is the blob spacing. When $c \rightarrow 0$, the interpolation kernel turns to the classical non-diffusion kernel. This modified interpolation kernel conserves the circulation of each vortex and also satisfies the conservation of linear and angular momentum of the vorticies.

The vortex method employs the viscous splitting procedure, where the vortex blobs are convected first and is then diffused through the remeshing process using the modified interpolation kernel. The advantage of this methodology is that the convection process is not constrained by the CFL condition. So, the convection time step size can be different than from the diffusion time step size and the diffusion time step size is a multiple of the convection time step size depending on the redistribution frequency $f_{redist}$. Therefore, the constrained that is imposed on the redistribution frequency is the stability bounds of the modified interpolation kernel. Analyzing the amplification factor and the phase error of the modified interpolation kernel in the Fourier space requires that the $c^2$ should be as follows:

$$\frac{1}{6} \leq c^2 \leq \frac{1}{2}. \tag{2.29}$$

This will ensure the stability of the problem and will suppress any spurious oscillations and ensure that it is a non-negative interpolation kernel with non-negative redistribution fractions.

### 2.3.3 Convergence study of the viscous vortex method

## 2.4 Boundary conditions at solid boundary

### 2.4.1 Boundary integral equations

#### Linked boundary conditions

### 2.4.2 Panel method for treating no-slip boundary condition

### 2.4.3 Convergence study of panel method

## 2.5 Simulation acceleration techniques

### 2.5.1 Fast multi-pole Method

### 2.5.2 Parallel computation in GPU

## 2.6 Validation of lagrangian method

### 2.6.1 Lamb-oseen vortex at $Re = 100$

### 2.6.2 Convection of Clercx-Bruneau dipole at $Re = 625$

## 2.7 Summary

Chapter 3

# Conclusion and Recommendation

## 3.1 Conclusion

### 3.1.1 Lagrangian domain

### 3.1.2 Eulerian domain

### 3.1.3 Hybrid method

## 3.2 Recommendations

### 3.2.1 Lagrangian domain

### 3.2.2 Eulerian domain

### 3.2.3 Hybrid method

# References

[1] L.a. Barba and Louis F. Rossi. Global field interpolation for particle methods. *Journal of Computational Physics*, 229(4):1292–1310, February 2010.

[2] J.Thomas Beale. On the Accuracy of Vortex Methods at Large Times. In Bjorn Engquist, Andrew Majda, and Mitchell Luskin, editors, *Computational Fluid Dynamics and Reacting Gas Flows SE - 2*, volume 12 of *The IMA Volumes in Mathematics and Its Applications*, pages 19–32. Springer New York, 1988.

[3] AJ Chorin. Numerical study of slightly viscous flow. *Journal of Fluid Mechanics*, 1973.

[4] G H Cottet and P D Koumoutsakos. *Vortex Methods: Theory and Practice*, volume 12. Cambridge University Press, 2000.

[5] S. Degond, P.; Mas-Gallic, Pierre Degond, and S Mas-Gallic. The weighted particle method for convection-diffusion equations. I. The case of an isotropic viscosity. *Mathematics of Computation*, 53(188):485–507, 1989.

[6] CJ Simão Ferreira. The near wake of the VAWT: 2D and 3D views of the VAWT aerodynamics. 2009.

[7] P Koumoutsakos. Inviscid axisymmetrization of an elliptical vortex. *Journal of Computational Physics*, 138(2):821–857, 1997.

[8] J.J Monaghan. Extrapolating B-splines for interpolation. *Journal of Computational Physics*, 60(2):253–262, September 1985.

[9] S. Shankar and L.van Dommelen. A New Diffusion Procedure for Vortex Methods. *Journal of Computational Physics*, 127(1):88–109, August 1996.

[10] Carlos Simão Ferreira, Gijs Kuik, Gerard Bussel, and Fulvio Scarano. Visualization by PIV of dynamic stall on a vertical axis wind turbine. *Experiments in Fluids*, 46(1):97–108, August 2008.

[11] Robert Speck. *Generalized algebraic kernels and multipole expansions for massively parallel vortex particle methods*, volume 7. Forschungszentrum Jülich, 2011.

[12] L.J. Vermeer, J.N. Sø rensen, and a. Crespo. Wind turbine wake aerodynamics. *Progress in Aerospace Sciences*, 39(6-7):467–510, August 2003.

[13] Daehyun Wee and Ahmed F. Ghoniem. Modified interpolation kernels for treating diffusion and remeshing in vortex methods. *Journal of Computational Physics*, 213(1):239–263, March 2006.

[14] Wikipedia. Vertical-Axis Wind Turbine, July 2013.